Measurement of Orbital Angular Momentum in Optical Tweezers

Simon J. W. Parkin, Timo A. Nieminen, Norman R. Heckenberg and Halina Rubinsztein-Dunlop

Centre for Biophotonics and Laser Science, School of Physical Sciences, The University of Queensland, QLD 4072, Australia.

ABSTRACT

Several techniques have been proposed and used for the rotation or alignment of microparticles in optical tweezers. In every case the optical torque results from the exchange of angular momentum between the beam and the particle, and, in principle, can be measured by purely optical means. Measurement of this torque could be useful for quantitative measurements in biological systems and is required to measure properties such as viscosity of liquids in microlitre (or less) volumes. Although elongated particles will align with the plane of polarisation, the torque efficiency is low, typically about $0.05\hbar$ per photon. The use of a beam with an elongated focal spot can increase this torque by a factor of 10-20 times, due to the transfer of orbital angular momentum. We report measurements of the orbital component using an analysing (Laguerre–Gauss) hologram. As a proof of principle experiment, an elliptical beam scattered off a glass rod was simulated on a macroscopic scale. The torque was found to be as much as $0.8\hbar$ per photon. Microscopic elongated objects have been aligned and rotated in optical tweezers and we plan to make measurements of the torques involved.

Keywords: Optical Tweezers, Orbital Angular Momentum, Holograms

1. INTRODUCTION

Optical tweezers are an optical trap produced by a laser beam that is tightly focused.[1] Some microscopic particles experience a gradient force towards this focus and can thus be trapped. Particles that are trapped are collected and held by the transfer of linear momentum from the laser beam to the particle. Rotation of the particle in the trap is made possible by the transfer of angular momentum (AM) from the incident laser beam. Both spin and orbital angular momentum of light have been used for rotation in optical tweezers.[2–5] Spin angular momentum, due to the polarisation of light, offers a maximum torque efficiency of $2\hbar$ per photon.[6, 7] The spin component has been used to rotate both elongated and birefringent particles[8–12]; with birefringent particles, the maximal $2\hbar$ per photon can be approached, but it is difficult to attain efficiencies much greater than $0.05\hbar$ per photon with elongated particles.[10] Orbital angular momentum allows for a much higher torque efficiency. Using an order l Laguerre–Gauss doughnut beam, $l\hbar$ per photon is available.[13] The azimuthal mode index, l, can be increased to allow strong torques to be applied to the trapped particle, relative to the available torque due to the polarisation of the beam.

Torque applied to particles in an optical trap by the light's polarisation has previously been measured by determining the degree of circular polarisation of the transmitted light from the optical trap.[14] However torque applied by the orbital component of optical AM has not been measured in an optical tweezers setup. A rotating elliptical beam can be used to apply a torque to a trapped elongated particle[15–17] and this transfer of AM comes from the orbital component of the beam. This is because the AM transfer between the beam and the particle is due to the intensity profile of the beam at the focus of the trap, and is independent of the polarisation of the beam. To quantify this torque, making it useful for measurements of biological or medical samples and also to complete the picture of torque in optical tweezers, this torque needs to be measured. The purpose of the experiments described in this paper is to make this measurement.

The measurement of orbital angular momentum, in this paper, is made by decomposing the beam into Laguerre–Gauss (LG) modes. Higher order LG modes are characterised by a helical phase front and contain

---

Further author information: Send correspondence to parkin@physics.uq.edu.au

a phase singularity in the centre of the beam. This means there is zero intensity in the centre of beam, and the resulting intensity distribution has earned the name: "doughnut" beam. Such beams carry orbital angular momentum and the amount is well defined.[13] LG modes can conveniently be produced using computer generated holograms.[18, 19] A hologram is the recording of an interference pattern generated by two light fields, one is the field of interest and the other is a reference field. The hologram can then be used to recreate the field of interest by illuminating the hologram with the reference field. A hologram can also be made by calculating the interference pattern from two fields and creating an image of this pattern that can be transferred to a holographic plate. This technique was used to create a hologram that produced an LG mode when illuminated by a Gaussian beam. In this paper this type of hologram is used to detect the orbital angular momentum in a laser beam.

A similar technique for detection has been used in the field of quantum information and communication. LG mode holograms (computer generated) can be used to produce superpositions of LG modes, and also to detect the mode of these states. These schemes propose to measure entanglement on the single photon level.[20, 21] However, while in this experiment we propose to measure the orbital angular momentum of an entire beam, the motivation to use and measure the orbital (rather than spin) component is similar. The infinite number of spatial modes offers multidimensional entanglement instead of just two states of polarisation. Likewise the orbital component offers greatly increased torque in optical tweezers by using high order LG modes, instead of the limited torque available from polarisation alone.

2. THEORY

The optical forces exerted by optical tweezers result from the transfer of momentum from the trapping beam to the particle by scattering. Similarly, optical torques arise from the transfer of angular momentum. That light and other electromagnetic fields can carry angular momentum follows directly from the transport of linear momentum, since the linear and angular momentum flux densities $\mathbf{J}$ and $\mathbf{p}$ are related by

$$\mathbf{J} = \mathbf{r} \times \mathbf{p} \tag{1}$$

where $\mathbf{r}$ is the position vector. For electromagnetic fields, the momentum flux density is given by

$$\mathbf{p} = \mathbf{S}/c = \mathbf{E} \times \mathbf{H}/c \tag{2}$$

where $\mathbf{S}$ is the Poynting vector and c is the speed of light. The coupled electric, $\mathbf{E}$, and magnetic fields, $\mathbf{H}$ form a spin-1 system, and, in general, (1) includes both a spin component, associated with the polarization, and an orbital component due to the spatial structure of the field.[22–24] Thus, we can write

$$\mathbf{J} = \mathbf{L} + \mathbf{S} \tag{3}$$

where the total angular momentum flux $\mathbf{J}$ is the sum of an orbital term $\mathbf{L}$ and a spin term $\mathbf{S}$. A similar relationship exists for the angular momentum flux at any point. The distinction is simply that the spin angular momentum density is independent of the choice of origin; that is, it is invariant with respect to translations of the coordinate system. Since the local conservation of angular momentum as the beam propagates in free space cannot depend on the choice of the origin of the coordinate system, both the orbital and spin components must be individually conserved, as well as the total angular momentum, since there would otherwise exist a choice-of-origin dependent torque exerted by the beam on free space. These quantities can only change if the field interacts with matter.[23]

In general, the separation into spin and orbital components is not quite as straightforward as one might hope.[22–24] One can, however, write expressions for the spin and orbital components. The Cartesian components of the time-averaged spin angular momentum flux density $\mathbf{s}$ are[22–24]

$$
\begin{aligned}
s_x &= \epsilon_0 \mathrm{Im}(E_y E_z^\star)/\omega \\
s_y &= \epsilon_0 \mathrm{Im}(E_x^\star E_z)/\omega \\
s_z &= \epsilon_0 \mathrm{Im}(E_x E_y^\star)/\omega
\end{aligned} \tag{4}
$$

where $E_{x,y,z}$ are the Cartesian components of $\mathbf{E}$, the complex vector amplitude. This result can also be written in terms of the Levi–Civita symbol as $s_i = i\epsilon_0\epsilon_{ijk}E_j E_k^\star/(2\omega)$, where the expression is summed over repeated indices and the real part is taken. The orbital components are[22–24]

$$l_i = i\epsilon_0 E_j(\mathbf{r} \times \nabla)E_j^\star/(2\omega). \tag{5}$$

These give simple results for paraxial beams. In the paraxial approximation, the two transverse vector components of the field de-couple, and the longitudinal component vanishes. Thus, the two linearly polarized components of the amplitude individually satisfy the scalar paraxial wave equation, and the spin and orbital angular momenta de-couple. The orbital angular momentum about the beam axis is conveniently found using the orbital angular momentum operator in cylindrical coordinates:

$$L_z = -i\partial/\partial\phi. \tag{6}$$

Notably, the Laguerre–Gauss modes are eigenfunctions of this operator, with eigenvalue l, the azimuthal mode index. Thus, the LG modes have a well-defined orbital angular momentum flux, and an LG modal decomposition of a beam is sufficient to determine the orbital angular momentum flux of the beam.

This can be used to calculate the torque exerted on an object by a paraxial beam. Assuming that both the incident and transmitted beam are known, an integral transform or an overdetermined least-squares fit using a set of matching points can be used to find the incident and transmitted LG modal decompositions, and the torque is then simply found. For the experiments described here, the incident beam profile is measured, and the transmitted beam profile is calculated by treating our test object as a pure phase object of negligible thickness altering only the phase of the incident beam as it passes through.[25]

Since the spin angular momentum depends on the polarisation of the field, an object that alters the polarisation of the beam has a reaction torque exerted on it by the field. Such torques can be used to rotate or align birefringent particles[8] or elongated particles of isotropic material.[10] While, in principle, a spin torque efficiency of up to $2\hbar$ per photon can be obtained, and high efficiencies can be readily obtained using birefringent particles, the spin torque exerted on elongated isotropic particles is much lower, with a typical maximum torque efficiency of about $0.05\hbar$ per photon.[10] Therefore, if larger torques are to be obtained, it is necessary to make use of the orbital angular momentum of light. One way in which this can be done is to use a beam with an elliptical focal spot—the elongated particle will tend to align with the elongated focal spot. As this effect does not depend on the polarisation of the beam, it is due to the transfer of orbital angular momentum. A rigorous electromagnetic calculation[26] of the optical torque exerted by an elliptical beam on an elongated object verifies that increased torques are obtained (figure 1).

3. METHOD

In this paper, we present two experiments designed to measure the orbital angular momentum component of a laser beam, and the torque applied by this beam to an object. The first experiment is designed to simulate, on a macroscopic scale, a situation in optical tweezers where an elongated object aligns with the major axis of an elliptical beam. The second experiment is to use optical tweezers to make a measurement of this situation described. In both experiments orbital angular momentum is detected by a hologram that generates LG modes of light. When a Gaussian beam is transmitted through the LG hologram, LG_{pl} modes are produced in the diffraction orders and each diffraction order has a different value for l. If we consider an LG_{pl} input beam of the same mode as the hologram, then a Gaussian (ie. LG_{00}) mode is observed in one of the first diffraction orders.[18, 21] If an arbitrary input beam strikes the hologram, then measuring the Gaussian component in each of the first diffraction orders determines the strength of the corresponding LG_{pl} mode in the input beam. The orbital angular momentum of a LG_{pl} mode is well defined and is $l\hbar$ per photon. Therefore we can determine the orbital angular momentum of some arbitrary beam.

In both experiments an elliptical beam is scattered off a phase object and we measure the change in the orbital angular momentum due to the object, hence we determine the torque exerted on the object. The phase object in the macro experiment is the image of a rod, developed onto a holographic plate. In the microscope, it
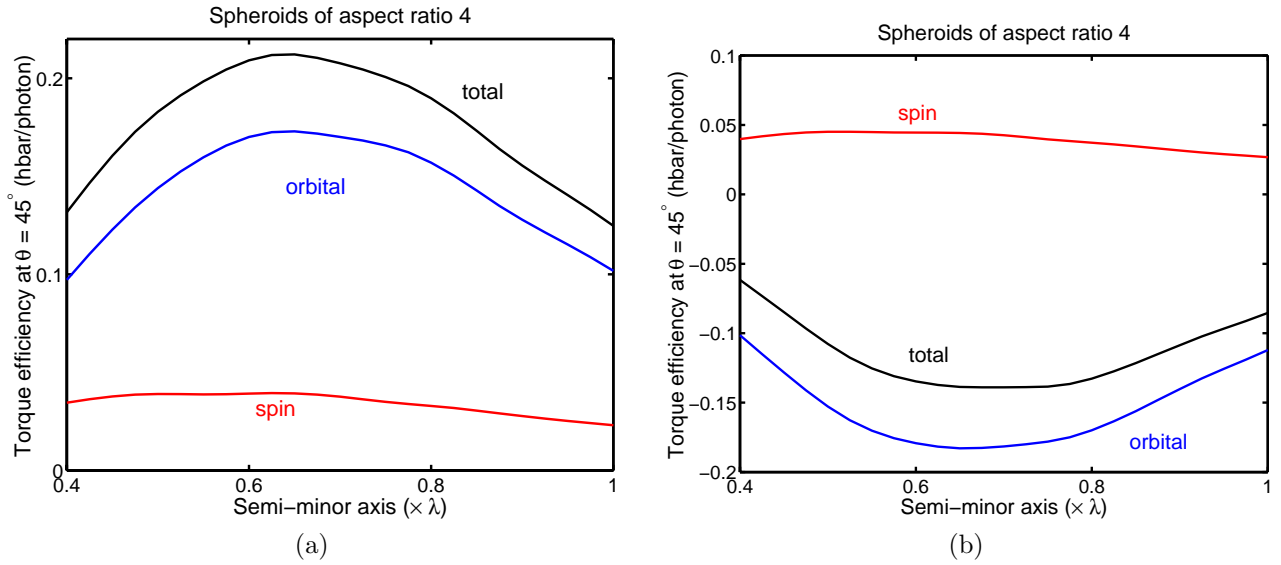
Figure 1. The theoretical torque on an elongated particle applied by the spin and orbital components of a beam's angular momentum. In the first case, (a) the polarisation is parallel with major axis of the elliptical beam, and in the second case (b) it is perpendicular.

is a glass rod a couple of microns in diameter. The elliptical beam can be decomposed into LG_{pl} modes, and as the beam scatters off the phase object the relative intensities of these modes will vary, marking a change in the orbital angular momentum of the beam. The rotational symmetry of the beam and the object means that the torque on the object will be predominately due to the $l = \pm 2$ modes.

In both of these experiments, two detection systems have been used to measure the strength of the Gaussian component in the first diffraction orders. The first method is to image the first diffraction orders onto a rotating screen and capture this image using a CCD camera. A centre pixel for each of the two diffraction orders is then determined. This is achieved by aligning a Gaussian beam with the LG_{pl} hologram and then locating the pixel with the minimum intensity at the centre of the two LG_{pl} modes imaged onto the screen. The intensity of this pixel is then proportional to the power in the mode with the appropriate angular momentum. The second method is to couple the two first diffraction orders into two single mode fibres and measure the intensity at the output of these fibres. Only the Gaussian component will propagate through the fibre, so the intensity of the light after the fibres is again proportional to the power in the mode with the appropriate angular momentum. The results from these methods were found to agree, so the first method using the CCD camera was used because of its simplicity and ease of use. Also the CCD camera gave a picture of the entire spot in the first diffraction orders, which helped in the alignment of the phase objects.

The holograms used in these experiments are computer generated. The interference pattern is calculated for plane waves, one carrying a phase singularity. The latter can be written in simple mathematical form as[19]:

$$E = E_0 \exp(iq\theta) \exp(-ikz) \tag{7}$$

where q is the charge of the singularity and θ is the angle transverse to the propagation of the field. The plane wave propagating at an angle to the LG mode field can be written as:

$$R = R_0 \exp(-ik_x x - ik_z z) \tag{8}$$

where k_x is the component of the propagation vector in the x dimension (k_z in the z dimension). If we let the plane of the hologram be at $z = 0$, then the interference pattern is represented as:

$$I = R_0^2 + E_0^2 + 2R_0 E_0 \langle \cos(k_x x - q\theta) \rangle. \tag{9}$$
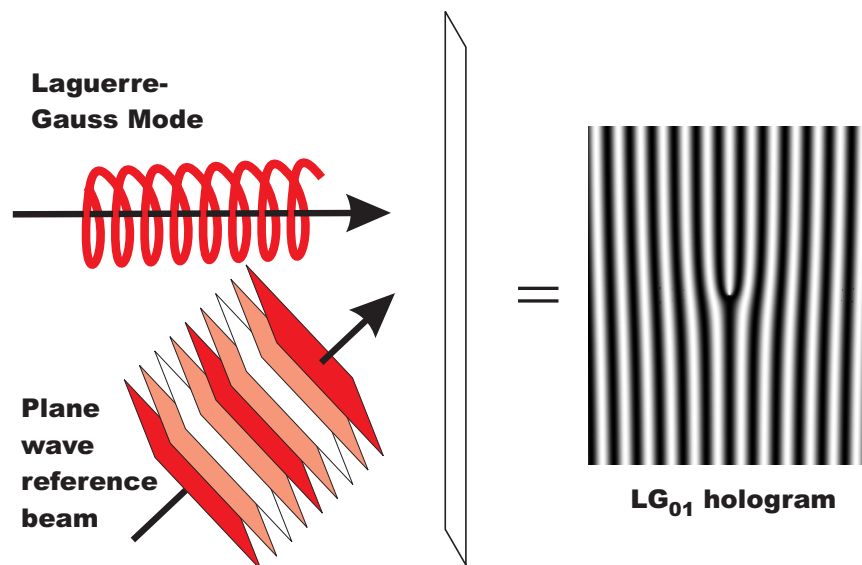
Figure 2. This figure shows the two beams used to calculate an LG_{01} hologram. A plane wave is the reference beam, and the field of interest is a LG_{01} mode which is off axis from the plane wave. The figure shows the helical phase front of the LG mode, and also the constant phase of the plane wave, with the phase varying only with time in the direction of propagation. When the hologram is illuminated with the reference beam (in practise a Gaussian beam) the LG_{01} mode and its complex conjugate ($LG_{0,-1}$) are produced in the first diffraction orders.
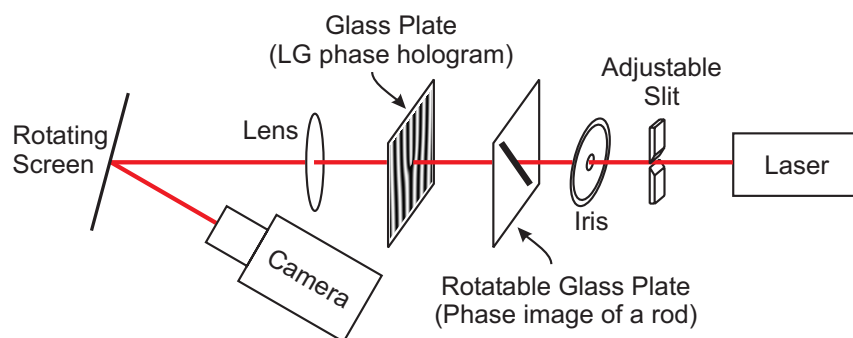

Figure 3. The experimental setup designed to measure the torque due to orbital angular momentum on a macroscopic phase object. A helium neon laser is used in this setup.

From this equation an image of the interference pattern is produced and an example is shown in figure 2. This image is transferred to Kodak technical pan film, which is a very fine grain black and white film, using a Polaroid ProPalette 7000 Digital Film Recorder. The recorder images to the 35mm film a 7 inch high resolution (4096×2732) CRT display, which combined with the fine grain of the film, gives a very high resolution image. The film is developed, and then contact printed to a holographic plate (made by GEOLA) with a fine grain silver halide emulsion layer. The plate is then developed and bleached using mercuric chloride. The phase thickness from a fringe maximum to minimum can be varied by varying the exposure time of the contact print process. This allows the efficiency of the hologram to be optimised. The phase objects (rods) used in the macro experiment were produced using the same method. Holograms fabricated with such a pattern actually produce beams which are superpositions of LG modes of varying index p, but with the same angular momentum index l. In the far field such beams are almost indistinguishable from pure LG_{0l} beams.[19]
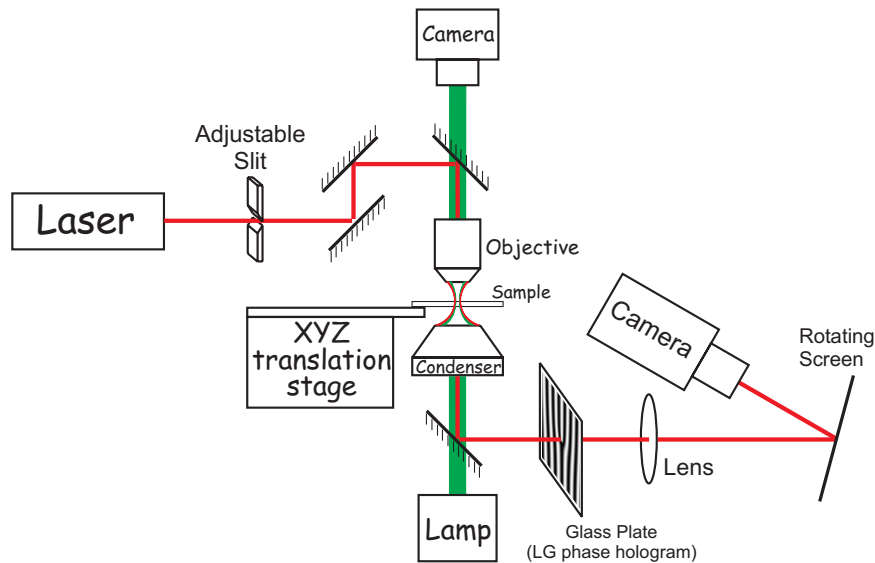
Figure 4. The optical tweezers setup used in the experiment designed to measure torque on microscopic elongated objects due to orbital angular momentum. A Neodymium-YAG laser is used in this setup.

The macroscopic experiment setup is shown in figure 3. A helium neon laser is used in this experiment, and an elliptical beam is generated using a slit. The adjustable slit actually produces a diffraction pattern, however the iris is used to select the zeroth order diffraction spot, which is elliptical. The elliptical beam is then directed through a glass plate which contains a phase image of a rod. The glass plate can be rotated about the axis of propagation of the beam, so that the rod can be orientated at any angle to the major axis of the elliptical beam. The beam is then directed towards a second glass plate which contains a LG_{02} sinusoidal phase hologram. The output of this hologram is then focused to a rotating screen, and the image is captured by a CCD camera. This hologram is called the analysing hologram, as combined with the CCD camera, it analyses the LG modal composition of the incoming beam and hence its orbital angular momentum.

The optical tweezers experiment is shown in figure 4. A CW Neodymium-YAG laser is directed towards an adjustable slit, which is mounted on a XY translation stage so that the slit can be centred on the beam. The slit can be rotated about the axis of propagation of the laser beam, and this rotation is driven by a computer controlled stepper motor. The beam is aligned with the microscope (objective and condenser) to allow optical trapping in the object plane of the microscope. The output beam from the condenser is directed onto a glass plate containing an LG_{02} phase hologram. The resulting diffraction pattern is focused to a rotating screen and the image is captured by a CCD camera. The rotatable slit allows trapped elongated objects to be rotated. This is because rotating the slit rotates the elliptical profile of the beam, so for the elongated particle to align itself with the major axis of the elliptical intensity profile at the focus of the optical trap, the particle must rotate as well. To make measurements of torque due to the angular momentum of the beam, a glass rod (about 1 μm in diameter) fixed to the microscope slide was used. The elliptical profile of the beam was then rotated about the glass rod, with the glass rod centred on the axis of rotation of the beam. This situation is similar to the macroscopic setup, where the phase image of the rod was rotated at different angle to the elliptical beam. In the microscopic case however, it is the beam that is rotated instead of the rod. The phase hologram at the output of the microscope, together with the CCD camera, then analyses the orbital angular momentum in the beam.

In both experiments the CCD camera detection system can be calibrated by removing the slit and the phase object from the setup and generating an LG_{02} beam for the input of the analysing hologram. This was done by inserting a second LG_{02} phase hologram into the setup and taking the first diffraction order, corresponding to the LG_{02} mode, as the input for the analysing hologram. This meant a pure LG mode with known power and a well defined orbital angular momentum was the input beam. For this case a 'filling in' of one of the first
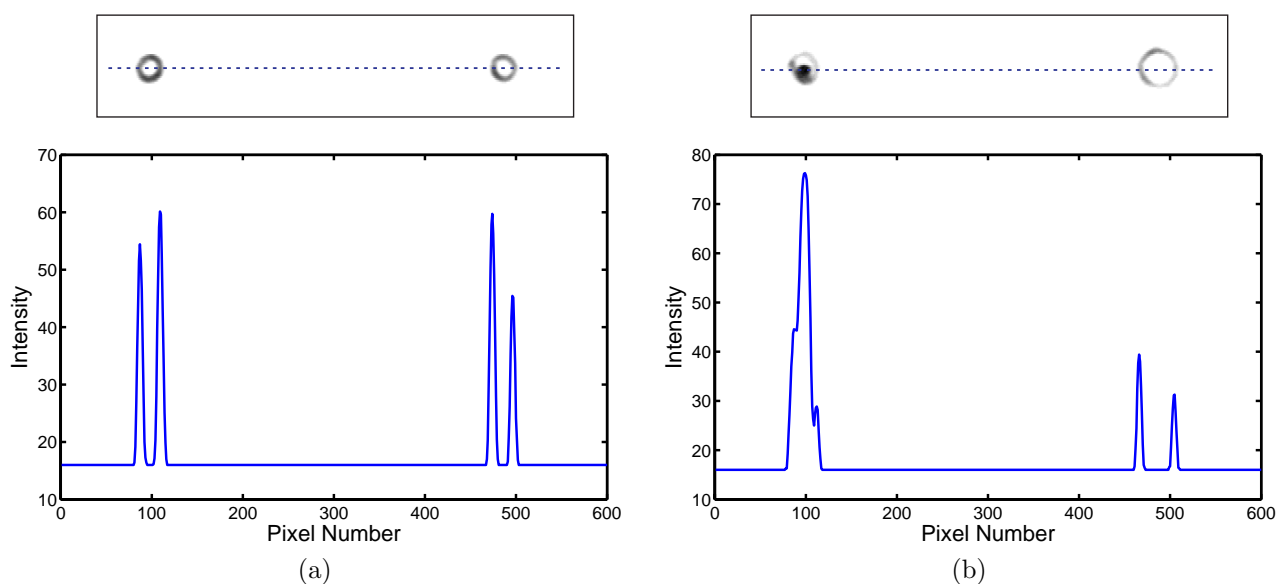
Figure 5. First diffraction orders from a LG_{02} phase hologram with (a) a Gaussian input beam, and (b) a LG_{02} mode input beam. The graphs show line scans through the image arrays. We see that in (a) two $LG_{0\pm2}$ modes were generated in the output of the hologram, and in (b) a Gaussian and a LG_{04} mode were generated in the output.

diffraction orders will occur so that a Gaussian spot is observed. The intensity at the peak of this Gaussian, which corresponds to the centre pixel that has already been located, was then associated with an input beam with $2\hbar$ per photon of orbital angular momentum. Therefore this intensity could then be compared to the intensity of this pixel when some arbitrary beam with unknown orbital angular momentum is the input beam of the analysing hologram. Note that the pattern obtained is the result of interference between the Gaussian component and others, so it is quite complex in general.

4. RESULTS

The following describes results from the macroscopic experiment. The calibration of the detection system first involved aligning the analysing hologram (LG_{02} phase hologram) to a Gaussian beam from the HeNe laser. The first two diffraction orders from this hologram are LG_{02} and $LG_{0,-2}$ modes and are shown in figure 5(a). The centre pixels on the CCD camera image were located using this image by finding the centre of each of the two vortices. An LG_{02} mode was was then used as the input beam and the resulting first two diffraction orders are shown in figure 5(b). We can see than one order 'fills in' to produce a Gaussian beam, while the the other order becomes a higher order LG mode. Therefore we see that a Gaussian component in the diffraction orders is an indication of an input beam with orbital angular momentum.

Once the detection system was calibrated, the simulation of an elongated object in optical tweezers was run. The elliptical beam was generated using an adjustable slit and the beam is then scattered by a phase image of a rod, which is at an angle to the major axis of the elliptical beam. The incident beam carries no net angular momentum. Angular momentum is generated in the beam as a torque is applied to the rod by the beam. This is because a torque acts to align the axis of the rod with major axis of the beam's elliptical profile. The detection system can measure this torque by monitoring the intensity of the two centre pixels. The difference in the signals at these two pixels is a measure of the orbital angular momentum within the beam. This difference is shown in figure 6 for the rod rotated at many different angles to the major axis of the elliptical beam. The signal difference shows a sinusoidal variation with angle which agrees with the theoretical curve. The period of this variation is twice that of a full rotation of the rod, as expected due to the two-fold symmetry of the beam and the rod. In the figure the signal is given as a torque efficiency with units of $\hbar$ per photon.
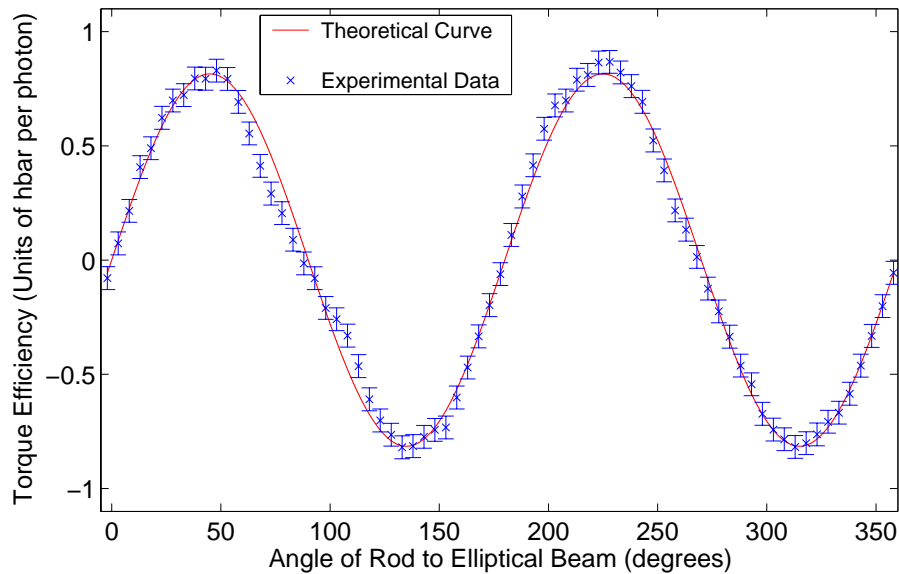
Figure 6. The torque efficiency applied by an elliptical beam to a rod, for different angles between the elongated axis of the rod and the major axis of the elliptical profile of the beam. The signal is the difference between the intensities of two pixels on a CCD camera corresponding to the centres of the first two diffraction orders.

The torque on the phase image of the rod is also dependent on the phase thickness of the rod. Rods with different phase thicknesses were produced by varying the contact print exposure time during the production of the phase image plates. The phase thickness of these rods was then measured using a Michelson interferometer that produces an image of the rod on a screen, overlayed by the interference pattern generated by the two arms of the interferometer. This image was captured by a CCD camera and the fringe shift was measured to determine the phase thickness of the rods. Each of these rods (one at a time) were aligned at an angle to the major axis of the elliptical beam corresponding to the position giving the maximum torque signal. It can be seen from figure 6 that this angle is 45 degrees to the major axis of the beam (this angle is equivalent to 135, 225 and 315 degrees). The torque efficiency as a function of phase shift was then found and the result is shown in figure 7 together with a theoretical curve. The theoretical curve is calculated using the methods described in the theory section of this paper.

In the optical tweezers experiment, an elliptical beam was used to apply a torque to a small piece of glass fibre. As this torque is independent of the polarisation of the beam, and due only to the intensity profile of the focal spot in the optical trap, then orbital angular momentum transfer is responsible for the rotation of the glass fibre. Figure 8 shows a glass fibre that has been rotated by turning the slit that creates the elliptical spot. The rod rotates anti-clockwise during the eight frames shown in the figure. This experiment demonstrates orbital angular momentum transfer in optical tweezers. Our future aim is to measure this torque using the techniques described for the macroscopic experiment.

5. CONCLUSION

The macroscopic experiment demonstrated that the orbital angular momentum of light could be measured using the techniques described in this paper. The transfer of this angular momentum resulted in torque efficiencies of as much as $0.8\hbar$ per photon. These results agreed well with the theoretical predictions. The transfer of this momentum was demonstrated in optical tweezers by using a rotating elliptical beam (generated by a rotating slit) to rotate glass rods in the focus of the optical trap. To measure this torque we proposed a technique similar to that used in the macroscopic experiment, which uses a LG phase hologram and CCD camera to determine the modal composition of the beam and hence infer the orbital angular momentum transferred to an object in
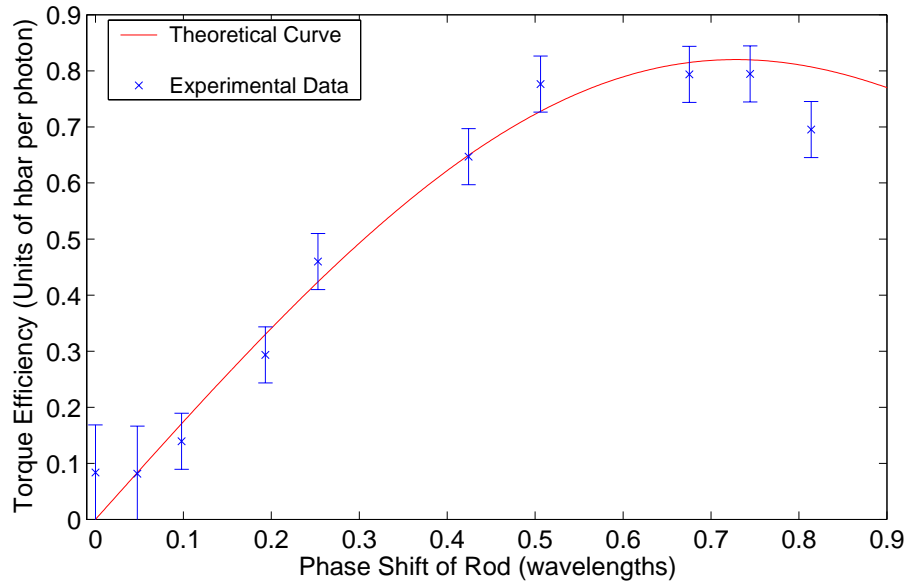
Figure 7. The torque efficiency applied by an elliptical beam to a rods with different phase thicknesses. The angle between the rods' elongated axis and the major axis of the elliptical profile of the beam is 45 degrees.
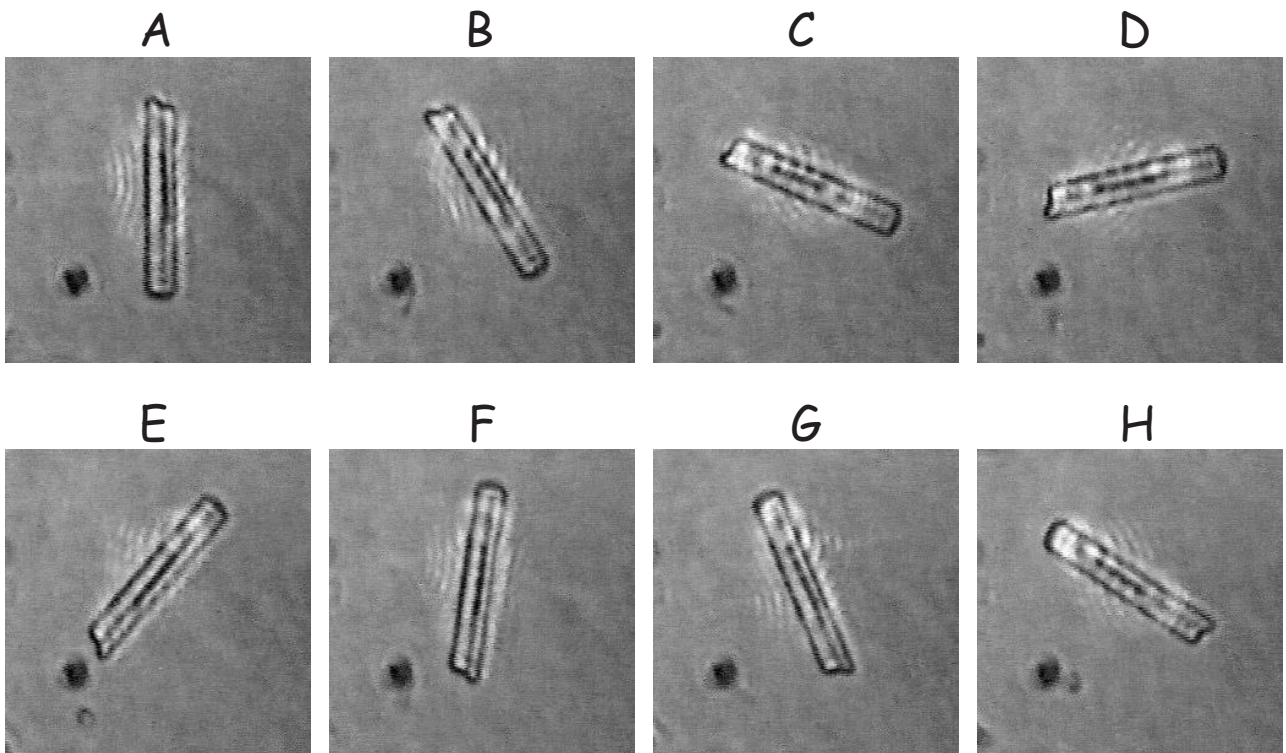

Figure 8. Rod rotated in an anticlockwise direction according to the sequence from A through to H.

the beam's path. To date this technique has been problematic in the optical tweezers setup, and we believe this is due to the elliptical beam rotating off the axis of propagation of the beam. One solution to this problem is to keep the elliptical beam's orientation fixed and instead rotate the fixed glass rod with respect to the beam. This can be achieved by using a rotating microscope stage with the axis of rotation centred on the focal spot of the trapping beam. This approach proved to be successful in the macro experiment.

REFERENCES

1. A. Ashkin, J. M. Dziedzic, J. E. Bjorkholm, and S.Chu, "Observation of single-beam gradient force optical trap for dielectric particles," *Optics Letters* **11**, p. 288, 1986.
2. H. He, M. E. J. Friese, N. R. Heckenberg, and H. Rubinsztein-Dunlop, "Direct observation of transfer of angular momentum to absorptive particles from a laser beam with a phase singularity," *Physical Review Letters* **75**, p. 826, 1995.
3. M. E. J. Friese, J. Enger, H. Rubinsztein-Dunlop, and N. R. Heckenberg, "Optical angular-momentum transfer to trapped absorbing particles," *Physical Review A* **54**, p. 1593, 1996.
4. M. E. J. Friese, T. A. Nieminen, N. R. Heckenberg, and H. Rubinsztein-Dunlop, "Optical torque controlled by elliptical polarization," *Optics Letters* **23**, pp. 1–3, 1998.
5. N. B. Simpson, K. Dholakia, L. Allen, and M. J. Padgett, "Mechanical equivalence of spin and orbital angular momentum of light: an optical spanner," *Optics Letters* **22**, p. 52, 1997.
6. J. H. Poynting, "The wave motion of a revolving shaft, and a suggestion as to the angular momentum in a beam of circularly polarised light," *Proceeding of the Royal Society of London* **82**, p. 560, 1909.
7. R. A. Beth, "Mechanical detection and measurement of the angular momentum of light," *Physical Review* **50**, p. 115, 1936.
8. M. E. J. Friese, T. A. Nieminen, N. R. Heckenberg, and H. Rubinsztein-Dunlop, "Optical alignment and spinning of laser-trapped microscopic particles," *Nature* **394**, pp. 348–350, 1998.
9. E. Higurashi, R. Sawada, and T. Ito, "Optically induced angular alignment of birefringent micro-objects by linear polarization," *Applied Physics Letters* **73**, pp. 3034–3036, 1998.
10. A. I. Bishop, T. A. Nieminen, N. R. Heckenberg, and H. Rubinsztein-Dunlop, "Optical application and measurement of torque on microparticles of isotropic nonabsorbing material," *Physical Review A* **68**, p. 033802, 2003.
11. S. Bayoudh, T. A. Nieminen, N. R. Heckenberg, and H. Rubinsztein-Dunlop, "Orientation of biological cells using plane-polarized gaussian beam optical tweezers," *Journal of Modern Optics* **50**, p. 15811590, 2003.
12. K. D. Bonin and B. Kourmanov, "Light torque nanocontrol, nanomotors and nanorockers," *Optics Express* **10**, pp. 984–989, 2002.
13. L. Allen, M. W. Beijersbergen, R. J. C. Spreeuw, and J. P. Woerdman, "Orbital angular momentum and the transformation of laguerre-gaussian laser modes," *Physical Review A* **45**, p. 8185, 1992.
14. A. I. Bishop, T. A. Nieminen, N. R. Heckenberg, and H. Rubinsztein-Dunlop, "Optical microrheology using rotating laser-trapped particles," *Physical Review Letters* **92**, p. 198104, 2004.
15. A. T. ONeil and M. J. Padgett, "Rotational control within optical tweezers by use of a rotating aperture," *Optics Letters* **27**, pp. 743–745, 2002.
16. E. Santamato, A. Sasso, B. Piccirillo, and A. Vella, "Optical angular momentum transfer to transparent isotropic particles using laser beam carrying zero average angular momentum," *Optics Express* **10**, pp. 872–878, 2002.
17. R. Dasgupta, S. K. Mohanty, and P. K. Gupta, "Controlled rotation of biological microscopic objects using optical line tweezers," *Biotechnology Letters* **25**, pp. 1625–1628, 2003.
18. N. R. Heckenberg, R. McDuff, C. P. Smith, H. Rubinsztein-Dunlop, and M. J. Wegener, "Laser beams with phase singularities," *Optical and Quantum Electronics* **24**, pp. S952–S962, 1992.
19. H. He, N. R. Heckenberg, and H. Rubinsztein-Dunlop, "Optical particle trapping with higher-order doughnut beams produced using high efficiency computer generated holograms," *Journal of Modern Optics* **42**, pp. 217–223, 1995.
20. A. Mair, A. Vaziri, G. Weihs, and A. Zeilinger, "Entanglement of the orbital angular momentum states of photons," *Nature* **412**, pp. 313–316, 2001.

21. J. Leach, M. J. Padgett, S. M. Barnett, S. Franke-Arnold, and J. Courtial, "Measuring the orbital angular momentum of a single photon," *Physical Review Letters* **88**, p. 257901, 2002.

22. J. Humblet, "Sur le moment d'impulsion d'une onde électromagnétique," *Physica* **10**, pp. 585–603, July 1943.

23. S. J. van Enk and G. Nienhuis, "Commutation rules and eigenvalues of spin and orbital angular momentum of radiation fields," *Journal of Modern Optics* **41**(5), pp. 963–977, 1994.

24. J. H. Crichton and P. L. Marston, "The measurable distinction between the spin and orbital angular momenta of electromagnetic radiation," *Electronic Journal of Differential Equations* **Conf. 04**, pp. 37–50, 2000.

25. S. J. Parkin, T. A. Nieminen, N. R. Heckenberg, and H. Rubinsztein-Dunlop, "Optical measurement of torque exerted on an elongated object by a noncircular laser beam," *To appear in Physical Review A* .

26. T. A. Nieminen, N. R. Heckenberg, and H. Rubinsztein-Dunlop, "Computational modelling of optical tweezers," *In this Volume* .